

A Theoretical Analysis of Acute Ischemia and Infarction Using ECG Reconstruction on a 2-D Model of Myocardium

A. Cimponeriu, C. Frank Starmer, and A. Bezerianos*

Abstract—We developed a two-dimensional ventricular tissue model in order to probe the determinants of electrocardiographic (ECG) morphology during acute and chronic ischemia. Hyperkalemia was simulated by step changes in $[K^+]_{out}$, while acidosis was induced by reducing Na^+ and Ca^{2+} conductances. Hypoxia was introduced by its effect on potassium activity. During the initial moments of ischemia, ECG changes were characterized by increases in QRS amplitude and ST segment shortening, followed in the advanced phase by ST baseline elevation, T conformation changes, widening of the QRS and significant decreases in QRS amplitude in spite of an enlarged Q. During each phase, potential proarrhythmic mechanisms were investigated. The presence of unexcitable regions of simulated myocardial infarction led to polymorphic ECG. We also observed a nonuniform deflection of the ST segment from beat to beat. We used similar protocols to explore the responses of infarcted myocardium after impairment resolving. We found that despite irreversible uncoupling of the necrotic region, the restored normal ionic concentrations produced an isopotential ST segment and monomorphic ECG complexes, while an enlarged Q wave was still visible. In summary, these numerical experiments indicate the possibility to track in the ECG pathologic changes following the altered electrophysiology of the ischemic heart.

Index Terms—Enlarged Q, infarction, ischemia, pointed T, polymorphic ECG, QRS amplitude, ST deflection, theoretical ECG.

I. INTRODUCTION

DESPITE amazing advances in medicine in the past years, recent statistics reveal that heart failure is still number one cause of mortality in the western countries, surpassing easily cancer [1]. In the majority of the cases, heart failure has the origin in an impairment of ventricular function, which in two-thirds of the cases is caused by a coronary artery disease like ischemia [1]. Although intensively studied especially in the last

Manuscript received July 23, 1999; revised July 20, 2000. This work was supported in part by the Greek Secretariat of Research and Technology under the PENEDE program (project 99ED146). The work of A. Cimponeriu was supported by the State Scholarships Foundation (S.S.F.) of Athens—Greece. The work of C.F. Starmer was supported by the Fulbright Program in Greece. Asterisk indicates corresponding author.

A. Cimponeriu is with the University of Patras, School of Medicine, Department of Medical Physics, 26500 Rion-Patras, Greece.

C. F. Starmer is with the Departments of Biometry/Epidemiology and Medicine (Cardiology), Medical University of South Carolina, Charleston, SC 29401 USA.

*A. Bezerianos is with the University of Patras, School of Medicine, Department of Medical Physics, 26500 Rion-Patras, Greece (e-mail: bezer@patras.upatras.gr).

Publisher Item Identifier S 0018-9294(01)00133-1.

two decades, many phenomena associated with ischemia are not yet well understood. Theoretical studies and animal heart experiments were carried out, independently and in parallel, to study wave propagation in ischemic myocardium [2], the altered conduction of ion channels [3], [4], mechanism of re-entry [5], [6] and spiral wave formation [7].

Most of the phenomena associated with the acute phase of ischemia rarely appear in a setting convenient for clinical investigation [8] and the complex modifications induced at the cellular level are difficult to be evaluated correctly at bedside because of the modulation induced by the autonomic nervous system and metabolic influences. Although not an infallible method, theoretical modeling has a clear advantage over the experimental study due to the possibility to manipulate individual parameters (conductivities, concentrations, etc.) separately or in combination, making easier to identify the origin of different electrical changes.

In this study, the electrophysiological and ionic mechanisms at ischemic cell and tissue level are explored using a simple model. Starting from Luo-Rudy I (LR I) cellular formulation [9] we built a two-dimensional (2-D) model of cardiac cells. Although a newer version of this cellular model exists [10], [11], adding the contribution of the recent patch-clamp data [12], we preferred the first one in our simulations. The choice was based on a balance between accurate representation of cell electrophysiology and reasonable computational load [13]. In addition, the LR I model performs, to our surprise, extremely well in simulating most of the complex changes associated with ischemia. Infarction was simulated by defining a necrotic region in the 2-D layer uncoupled from the normal myocardium by an injured transitional band. For clinical-like evaluation of the results in both acute and chronic ischemia, the theoretical electrocardiographic (ECG) signal was reconstructed. “Recordings” were made during normal and acute ischemic conditions, infarction and after impairment resolving when despite of necrotic region presence the chemical concentrations have returned to normal levels.

II. METHODS

A. Ventricular Cell Model

The starting point in our investigation of ischemia is the Luo-Rudy I ventricular cell model [9]. Based mainly on data taken from guinea-pig hearts, this model, following mathematically the Hodgkin-Huxley formalism [14], is used to study the electrical activity of a general mammalian ventricular cell.

The equation governing the electrical activity of the stimulated cell can be written

$$C \cdot \frac{dV}{dt} = -I_{\text{ionic}} + I_{\text{stim}} \quad (1)$$

where

C membrane capacitance;

V transmembranal potential;

I_{ionic} the ionic current;

I_{stim} stimulation current injected during excitation.

A membrane specific capacitance of $1 \mu\text{F}/\text{cm}^2$ and resting membrane potential of -85 mV were considered. The cell was stimulated by “injecting” a current pulse of $50 \mu\text{A}/\text{cm}^2$ (the experimented threshold value was $43.4 \mu\text{A}/\text{cm}^2$) and 0.5-ms duration. The differential equations used for computing the ionic currents involved in the model were solved using combined Euler (explicit) and implicit methods. The less resource consuming method (explicit) was generally implemented, using the more accurate and stable implicit algorithm only for the fast time-constant components (like sodium activation process). In this way a $125\text{-}\mu\text{s}$ ($1/8 \text{ ms}$) time integration step was enough to obtain a stable algorithm.

The most important factor altering the electrical activity of the heart during early ischemia is the intracellular loss and the consequent extracellular accumulation of potassium ions, known as hyperkalemia [15], [16]. Acidification and hypoxia are the other major pathological conditions manifesting during ischemia. Accounting on nonelectrical cellular changes, these two phenomena are quite difficult to simulate in an electrical model. Based on the experimental results, the two conditions were introduced in the model by altering electrical parameters. The main effect of hypoxia is thought to be the activation of the adenosine triphosphate (ATP)-sensitive potassium channels, practically closed during normal conditions. One of the results is the increased extracellular potassium level. We preferred tuning this parameter to simulate partially hypoxia, instead of adding new equations in the cellular model. Another reason of not using the ATP-sensitive potassium current in our model is justified by the fact that it has not been confirmed yet whether the associated channels actually open during the early phase of ischemia or not [17], [18]. During acidosis, both intracellular and extracellular pH are known to affect the function of several ionic channels. Sodium and calcium channels were observed to be affected by a drop in their specific conductances by 25% to 50% during the first 10 min of ischemic episode (corresponding to one unit drop in pH value) [19]. We simulated the effect of acidification by considering a fixed sodium conductance 25% smaller than the normal value and a calcium conductance having 50% of its original value.

Inducing the mentioned pathological conditions individually or in combination, we investigated the electrical response of the ischemic cell. Cell excitability was studied by measuring at each step the action potential (AP) amplitude, AP maximum up-stroke velocity and sodium current peak amplitude. We also evaluated the resting membrane potential, AP duration and cell refractory period.

B. Two-Dimensional Model of the Ventricular Myocardium

The myocardium, generally, consists of muscle fiber cells connected one by one through some low resistance “bridges”, called gap junctions [20], [21]. The structure of this “emergency tunnels” is similar with the ion channel morphology and seem to open in response to changes in membrane potential, so they might be voltage-gated. The junction provides continuity between the inner fluid of one cell and the other’s cell cytoplasm. In these circumstances, the gap junctions communicate membrane depolarization signals directly from one cell to the neighbors through the flow of charged ions. This structure resembles an interconnected network in which the mentioned mechanisms of transmission seem to help the myocardial contraction by co-ordinating the firing of all the cells with minimum delay. Implementing a 2-D model of the myocardial tissue is not an easy problem taking into account the complex morphology of the cardiac muscle. The nonuniform arrangement of cells is difficult to represent with high fidelity, but complex phenomena associated with heart electrophysiology were successfully analyzed even in a simple squared-grid arrangement of cells [2], [22]. This topology will be used here (Fig. 1), as the one who gives reasonable computational speed. On the other hand, this structure can be seen as a linear arrangement of electrical cables, similar with fiber arrangement in the myocardium. The cell-to-cell junctional impedance was taken to be purely resistive as we did not observe an improved accuracy of representation by considering a parallel capacitive component and there is no clear evidence that such component exists [23].

A 2-D model is a finite representation of the myocardium. Thus, the propagation of action potential in such a structure is implicitly affected by the presence of borders where the propagation velocity drops suddenly to zero due to an abrupt change in connective resistances. At these borders there is no current flowing out of the system, so the boundary conditions stated in this way are called no-flux boundary conditions. The sealed-end boundary conditions distort the propagating AP due to the impedance mismatch, so a 2-D structure of sufficient dimension should be implemented in order to observe a not-distorted propagation. This observation justifies partially our choice concerning the cellular formulation as the one that permitted to implement a relative large 2-D grid (200×200 cells).

The partial differential equation (PDE) describing the 2-D model includes, additional to cellular formulation, the spatial derivatives

$$C \cdot \frac{dV}{dt} = -I_{\text{ionic}} + \frac{1}{R_i} \cdot \left(\frac{\partial^2 V}{\partial x^2} + \frac{\partial^2 V}{\partial y^2} \right). \quad (2)$$

R_i being the cell-to-cell interconnecting resistance. This PDE can be re-written using finite differences as:

$$V_{ij}^{t+dt} = -dt \cdot I_{\text{ionic}} + q \cdot V_{i-1,j}^t + q \cdot V_{i+1,j}^t + q \cdot V_{i,j-1}^t + q \cdot V_{i,j+1}^t + (1 - 4 \cdot q) \cdot V_{ij}^t \quad (3)$$

where the notation

$$q = \frac{1}{R_i} \cdot \frac{dt}{dx^2} \quad (4)$$

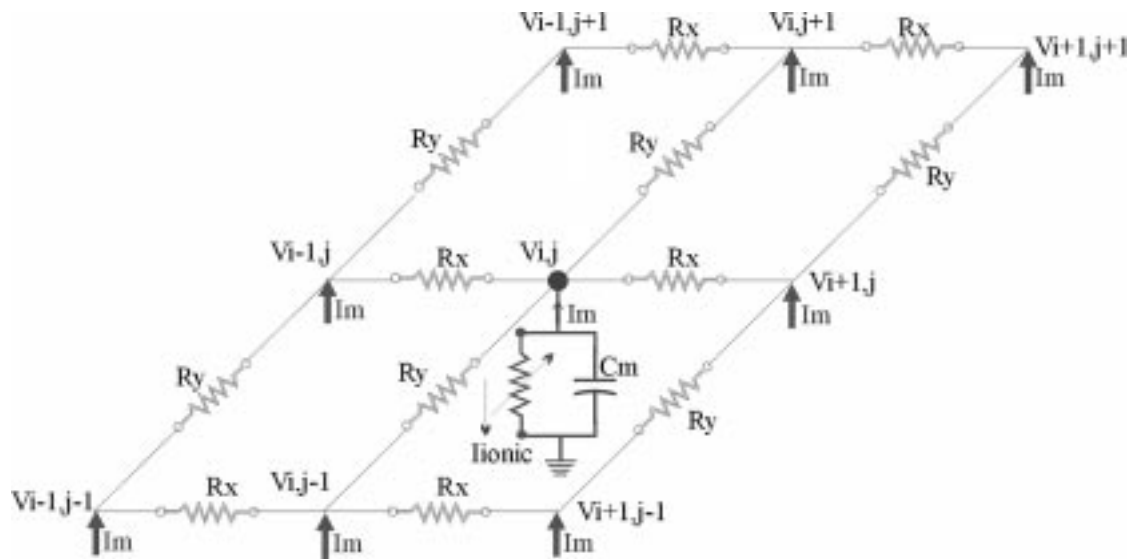


Fig. 1. Squared-grid arrangement of cells in the 2-D model of myocardium.

was used assuming an equal space integration step in the longitudinal and transversal direction $dx = dy$.

Despite of implementing an efficient integration algorithm it was difficult to carry out the simulations on a layer of more than 200×200 cells. This is, however, a more than satisfactory dimension as can be concluded from studies of related literature. Usually a 100×100 dimension is implemented and sometimes simplification of the space integration algorithm is used in order to reduce the computational load. The 2-D structure presented here took the advantage of a simple, yet realistic, cellular model which permitted an increase in the size of the simulated layer without affecting the precision of the integration algorithm, using a constant step along the whole spatial matrix.

Propagation was initiated by exciting one edge of the 2-D layer over a thickness of five cells, value exceeding in our simulation the liminal region. We employed an interconnecting effective axial resistance R_i lumped at cell-to-cell junction having a value of $200 \Omega \cdot \text{cm}$. We assumed that the interior of the cell is equipotential taking into account the negligible resistance of the cytosol compared with the interconnecting resistance. The spatial integration step used was $dx = 125 \mu\text{m}$ ($1/8$ mm) and the time integration step (dt) employed had a value of $62.5 \mu\text{s}$ ($1/16$ ms).

The propagation was analyzed during normal conditions and in a simulated myocardium partially or totally affected by acute ischemia. The alterations induced by hyperkalemia and hypoxia manifest mainly at the cellular level. Acidosis, however, has in addition to cellular changes, a macroscopic effect. The coupling of cells through gap-junctions is apparently affected by intracellular pH [15]. It was suggested that the fall in the internal pH value (acidic conditions) has cell-to-cell uncoupling effect. Usually these changes are nonreversible and lead to chronic alterations of the myocardium. The chronic phase was investigated defining a two-regions topology of the infarcted part of the myocardium: a necrotic area ($2 \text{ k}\Omega \cdot \text{cm}$ effective axial resistance) and a surrounding transitional band

of injured tissue ($1 \text{ k}\Omega \cdot \text{cm}$ effective axial resistance). This implies a two-steps change of the cell-to-cell interconnecting resistance from normal to necrotic region. This gives a more realistic representation of the infarcted myocardium as the abrupt uncoupling is not likely to manifest in the real tissue.

In order to evaluate the results from a clinical point of view, the theoretical ECG signal was reconstructed. To do this job in an efficient way a comparison with real myocardium was made: the real myocardium is a nonbounded, continuous structure and the ECG recording is not affected by boundary reflections. While for studying the propagation in the 2-D structure, simple stating the boundary conditions proved to be enough, the reconstruction of ECG on this structure was affected by artifacts due to finite dimension of the analyzed layer. When the propagating wave reaches the far end border the current does not have where to leak (no-flux boundary conditions) and the back recovery is delayed (behavior similar with conduction block). Thus, in that region the membrane is kept at higher potential until the second stimulus injects current in the tissue and initiates a new depolarization wave. This "clamp" of the membrane potential introduces unwanted changes in the theoretical ECG if the reconstruction takes place considering the whole structure. This observation led to the conclusion that the best way to reconstruct the signal is to consider a smaller region of the 2-D structure. In this way, the "external" recording sees the electrical field of the myocardium coming from a virtually nonfinite structure and the results are more closed to reality. This approach was considered simpler than building a continuous spherical structure, using the layer as envelope.

The ECG represents the electrical potential derived from the activation of cardiac tissue as a function of time, observed in one point situated at some distance from the heart. Using the volume conductor theory we computed the ECG by integrating the total membrane current (I_{membrane}), including the capacitive component ($C \cdot dV/dt$), weighted by the inverse of Euclidean distance between the 2-D layer and the remote observation point. If the observation point is defined by $P(x_p, y_p, z_p)$ and we con-

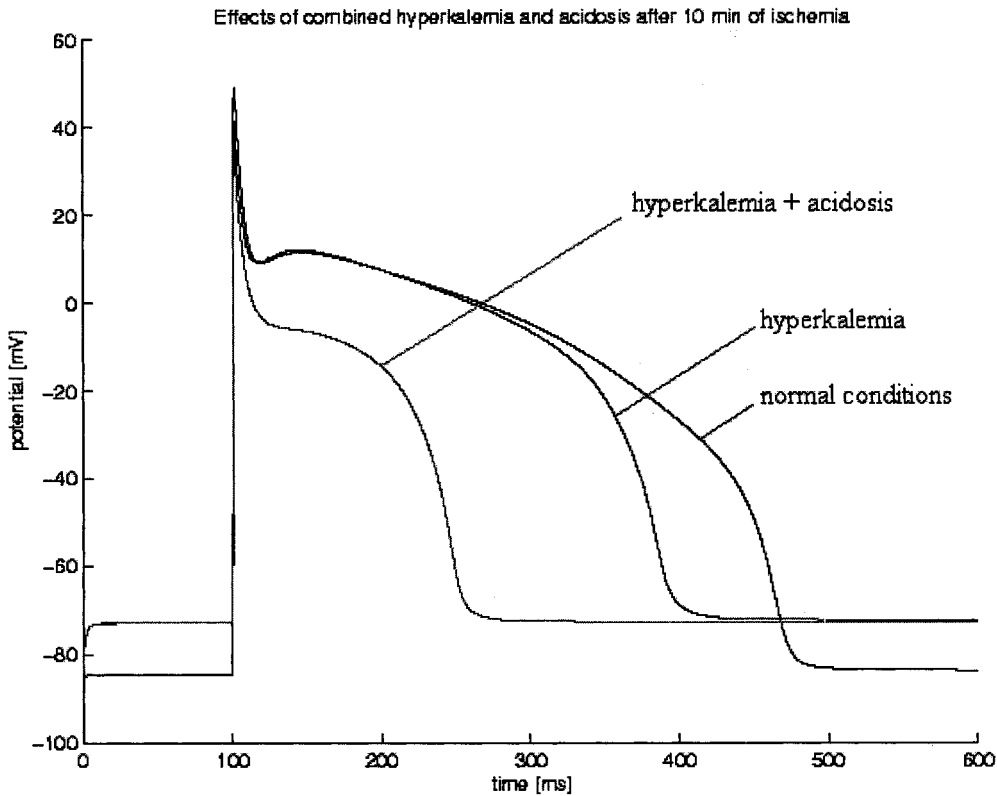


Fig. 2. Effects of hyperkalemia and acidosis on computed AP characteristics.

sider the plane of the tissue as reference level along the z axis ($z = 0$) then the electrical potential in that specific point can be written as

$$e(x_p, y_p, z_p) = \iint_{\text{surface}} \frac{I_{\text{membrane}}}{\sqrt{(x - x_p)^2 + (y - y_p)^2 + z_p^2}} dx dy \quad (5)$$

$$I_{\text{membrane}} = I_{\text{ionic}} + C \frac{dV}{dt} \quad (6)$$

where x and y are the coordinates of the current point of the integrated 2-D structure ($z = 0$). Three observation points were considered for building the Eindthoven triangle. Every pair of observation points defines one lead. For each lead described by the extremity points $P_1(x_{p1}, y_{p1}, z_{p1})$ and $P_2(x_{p2}, y_{p2}, z_{p2})$, the “projected” ECG signal is the potential difference

$$\text{ECG}(P_1, P_2) = e(x_{p1}, y_{p1}, z_{p1}) - e(x_{p2}, y_{p2}, z_{p2}). \quad (7)$$

A 60° orientation of the cardiac vector was considered when defining the leads [24]. In other words lead II is parallel with the direction of propagation under normal condition (homogeneous tissue, not affected by pathological changes). The electrodes coordinates were $P_1(20, 0, 20)$, $P_2(200, 90, 20)$ and $P_3(20, 180, 20)$ relative to the 200×200 layer. “Recordings” were taken during normal and ischemic conditions, including infarcted myocardium after impairment resolving when despite of necrotic region presence the chemical concentrations have returned to normal.

III. RESULTS

A. The Ischemic Cell

As we mentioned, our primary objective in this study was to use a simple, yet realistic, cellular formulation that permits ischemia analysis on relatively large 2-D structures. We chose the Luo-Rudy I [9] model as the one that offered the best compromise between the accurate physiological representation and computational load. We first tested the accuracy of this model in simulating such a complex phenomenon like ischemia. Despite of ATP sensitive potassium current lack (present in the up-dated Luo-Rudy II model [19]), this model still performed very well in simulating the ischemic conditions.

Alterations in extracellular potassium concentration at different levels of acute ischemia, induced in this model, change all main characteristics of the action potential. The major changes that can be observed are the elevated resting membrane potential and the shortening in action potential duration previously presented by [19] (not shown).

Fig. 2 shows the effect of 10 min of acute ischemia considering hyperkalemia alone ($[K^+]_{\text{out}} = 9 \text{ mM/l}$ [15]) and the more realistic representation of combined effects, hyperkalemia and acidosis corresponding to the same moment in time. Combined with hyperkalemia, acidosis produced in our simulations further decrease of the action potential duration. This is the result of shortening of the AP plateau phase due to reduced Ca^{2+} channels conductivity, demonstrated also by the simultaneous reduction in the plateau level. Not affecting significantly potassium activity, acidosis does not visibly influence the resting membrane potential.

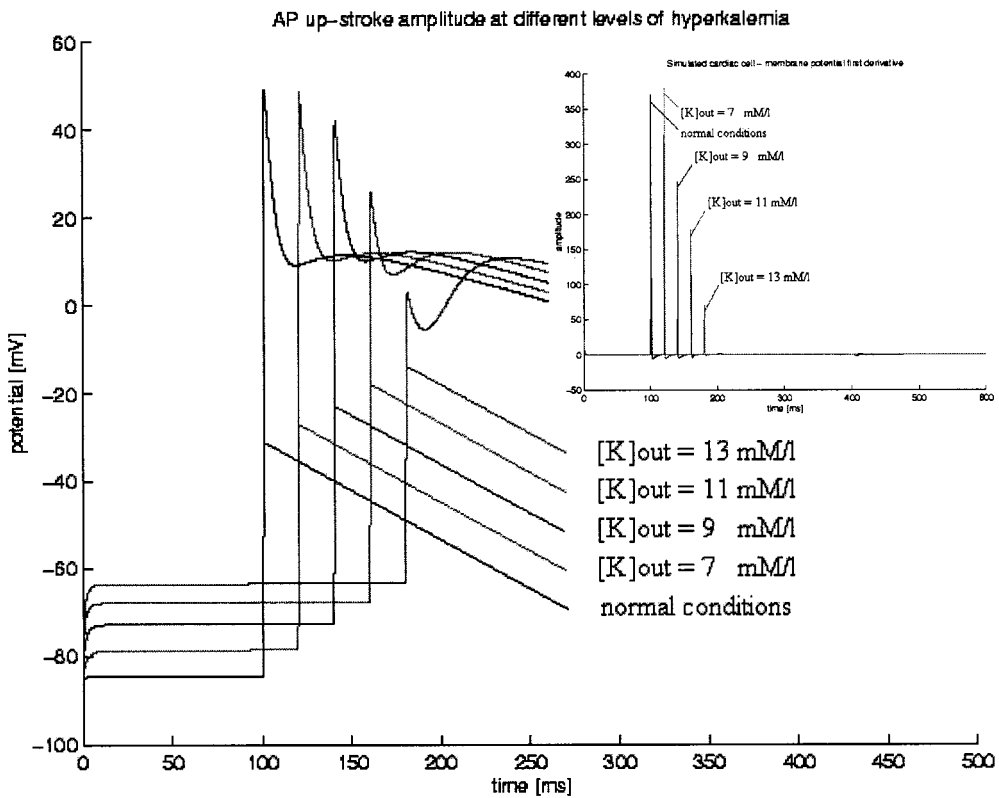


Fig. 3. AP up-stroke computed at different levels of hyperkalemia.

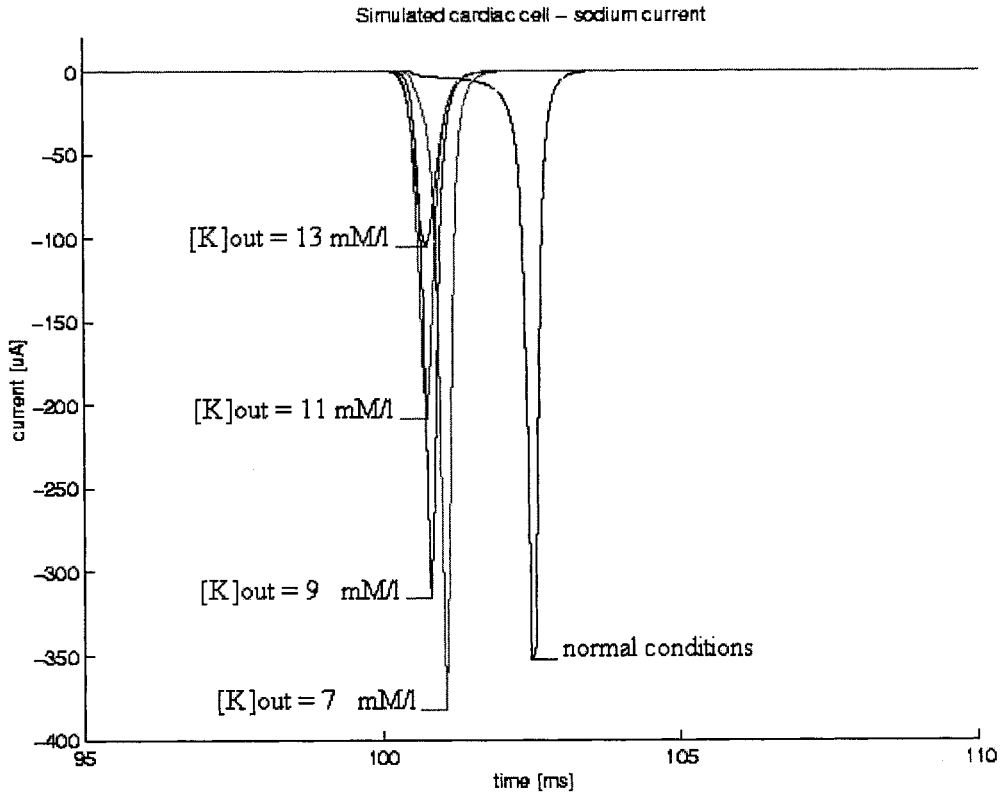


Fig. 4. Sodium current computed during acute ischemia.

Intracellular potassium concentration $[K^+]_{in}$ seems to be influenced (up to 14% decrease) [15] by acidosis, but the resulting membrane depolarization (3–4 mV) is small when comparing

with hyperkalemic effect. Although simulating this condition is not a problem, it was not considered important for our study, which is focused on cellular analysis of ischemia only partially.

Within minutes of coronary occlusion, experimental recordings showed a decrease in action potential amplitude and maximum up-stroke velocity (dV/dt_{\max}). As reported before in other studies [19], we observed from our simulations that cell excitability is not lost immediately after the occlusion. Fig. 3 shows the AP up-stroke for values of $[K^+]_{\text{out}}$ ranging from 5.4 mM/l to 13 mM/l. A stimulus of the same characteristics (50 $\mu\text{A}/\text{cm}^2$ amplitude and 0.5 ms duration) was in this case applied at different moments in time in order to separate the curves on the graphs. During early stages of ischemia (2–3 min after coronary occlusion when $[K^+]_{\text{out}}$ is situated around 7 mM/l [15]), the AP up-stroke is slightly increased (Fig. 3) and only later does the AP up-stroke starts to decrease. The partial depolarization of the membrane, in the first moments drives the cell closer to the threshold of Na^+ channel activation and the current requirement for excitation is reduced since $(V_{\text{rest}} - V_{\text{threshold}})$ is reduced with minimal changes in Na^+ channels availability. After further increase of the extracellular potassium concentration, the membrane reaches higher degree of depolarization and the excitability is diminished as a result of sodium channel inactivation. These observations are confirmed also by analyzing the AP maximum up-stroke velocity (Fig. 3—right corner).

The initiation phase of the action potential (the up-stroke) accounts on fast sodium current response. We explored the changes in sodium current during acute ischemic conditions (Fig. 4) by injecting a stimulus current of the same amplitude (50 $\mu\text{A}/\text{cm}^2$) and time characteristics (0.5 ms duration, 100 ms moment of excitation) in the normal and ischemic cell. During normal conditions our results display a 2–3 ms initiation delay of the sodium current peak. Membrane depolarization during acute ischemia accelerates the response of the sodium channels as the membrane is situated closer to the threshold. At early stages ($[K^+]_{\text{out}} = 7 \text{ mM/l}$) the sodium current peak amplitude is higher as the sodium channels are not yet affected by the inactivation process and the membrane requires less current to be injected in order to compensate the difference $V_{\text{rest}} - V_{\text{threshold}}$. The almost instantaneous response of the Na^+ channels at higher levels of hyperkalemia, however, is not a sufficient condition for generating larger sodium current, as the channels inactivation becomes the dominating factor. The response of the ischemic cell shows a shift from fast sodium-based to a slow calcium-based up-stroke (Fig. 3).

Exploration of cell refractoriness during acute ischemia led to convergent results concerning cell excitability (Fig. 5). The cell was excited using the procedure already mentioned, applying an additional test stimulus at the firing limit for the normal cell, following a protocol widely employed experimentally [15]. At different hyperkalemic levels the stimulus location and characteristics were maintained. Despite shortening of the action potential during ischemia, it was demonstrated that the refractory period was prolonged as a result of extracellular potassium accumulation [19]. However, the membrane response for $[K^+]_{\text{out}} = 7 \text{ mM/l}$ leads to observation that the early ischemic cell is not refractory to the second stimulus and manifests an increased response. This is the result of increased excitability that we observed during AP up-stroke analysis. These observations serve as an explanation for increasing the probability of early reen-

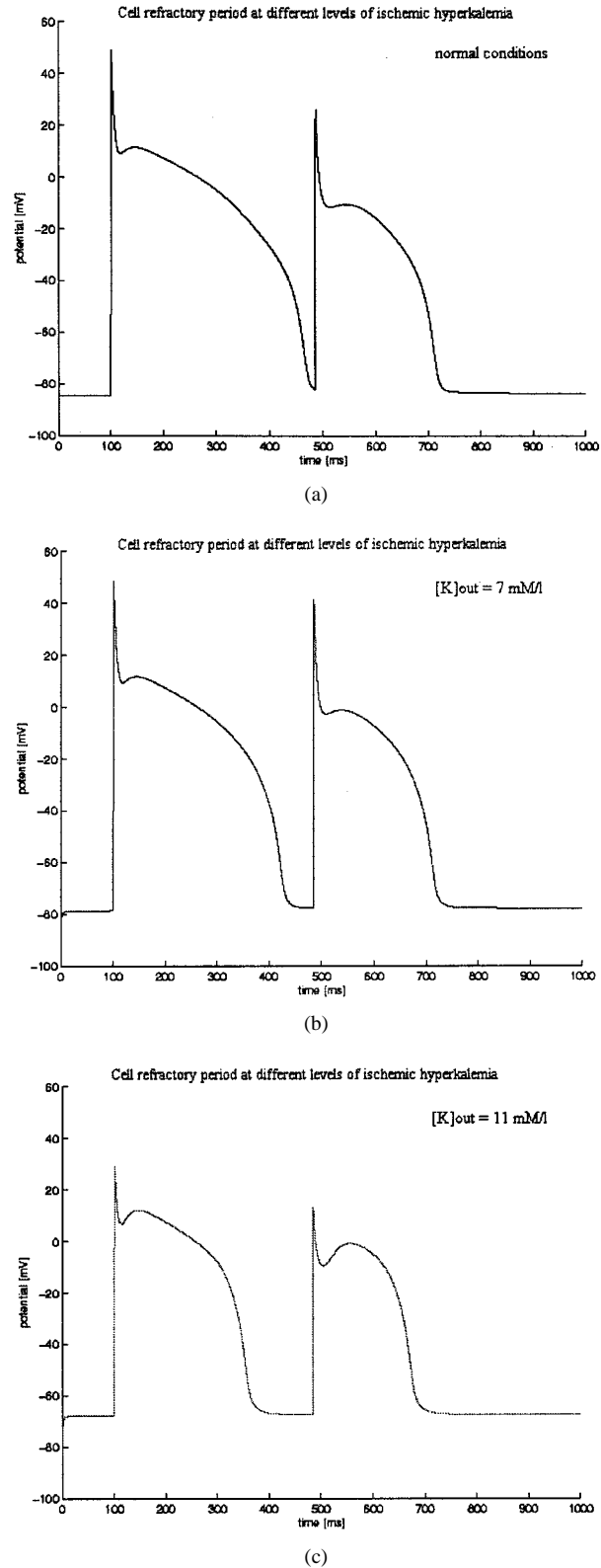


Fig. 5. Cell refractoriness during simulated acute ischemia.

trant arrhythmias during ischemia (known also as phase 1a ventricular arrhythmias [8]) and were analyzed in the 2-D study. At higher $[K^+]_{\text{out}}$, however, due to the elevated resting membrane potential, the channels recovery process is slowed down and the cell becomes more refractory to the second stimulus.

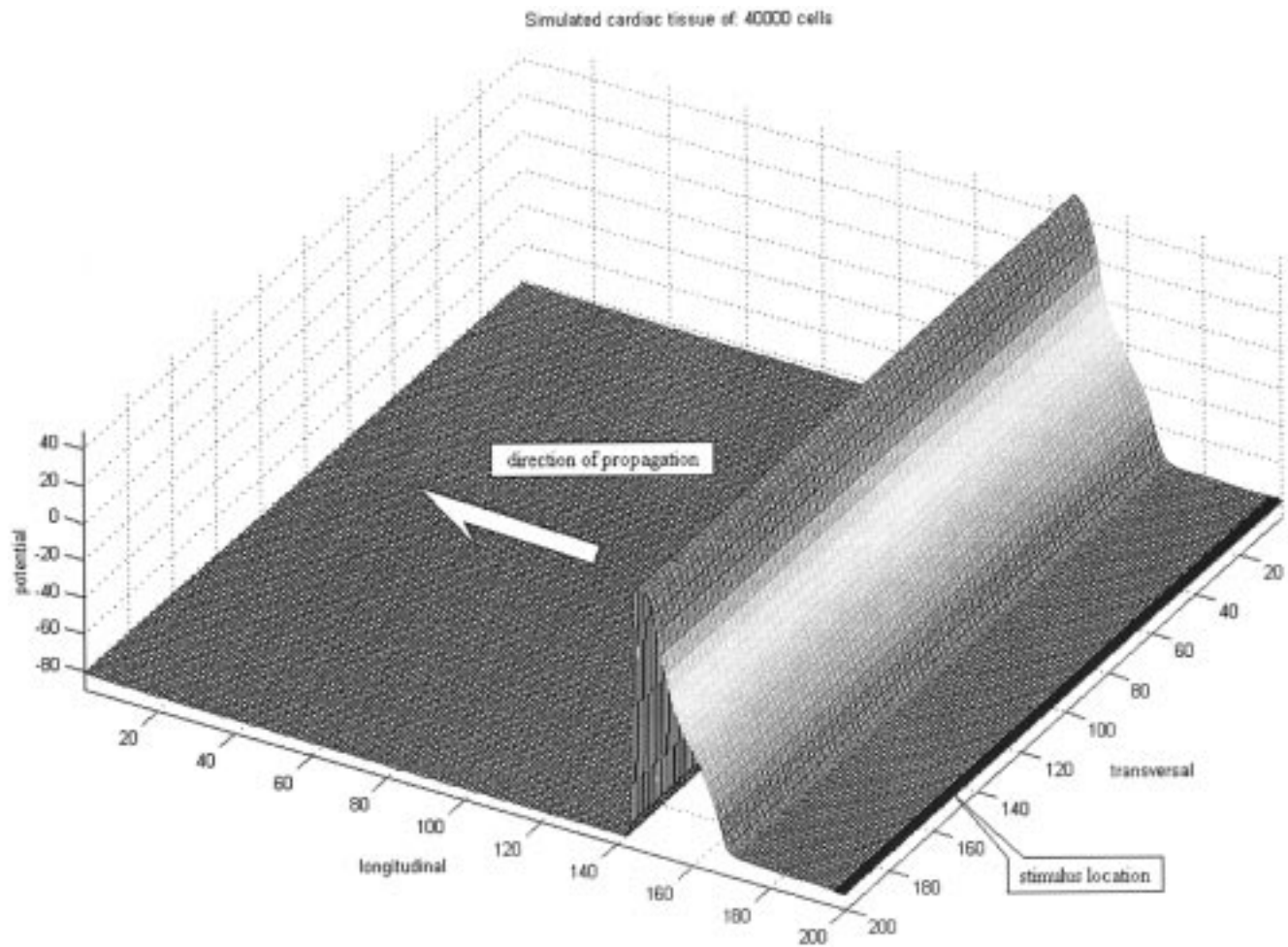


Fig. 6. Depolarization wave propagation in the simulated normal myocardium.

B. The 2-D Model of the Ischemic Myocardium

Fig. 6 shows a normal propagating depolarization wave simulated using our modeled 2-D structure. The “investigated tissue” was excited over a whole edge by an initial clamp of the membrane potential to +30 mV over a band of five cells. For simplicity reasons, the coupling resistances in the longitudinal and transversal direction were considered equal (200- $\Omega\cdot\text{cm}$ effective value).

In order to analyze the propagation of action potential during early stages of acute ischemia we induced the conditions of hyperkalemia, using a gradual distribution of chemical alterations over the modeled tissue. A small region of the myocardium was affected by hyperkalemia and the excitation was applied on the same side of the 2-D layer in the nonaffected portion (half of the edge) of the simulated ventricular tissue (Fig. 8).

The differences in propagation velocity, due to nonuniform excitability of the myocardium [22], create a visible tendency of re-entry at the interface normal region—pathological tissue. This phenomenon is more obvious in the initial phase of ischemia [Fig. 8(a)] as we expected in the cellular study and is directly related with the increased excitability and faster recovery. Under these circumstances, the depolarization wave front is virtually able to re-excite the ischemic part, creating the proper condition for spiral waves formation and life threatening ar-

rhythmias. At higher values of potassium in the extracellular space [Fig. 8(b)], although the phenomenon is still visible, the vulnerability of the ischemic region to re-excitation is diminished by the longer refractory period. The propagation difference can be analyzed in Fig. 8 where concentrations of potassium of seven, respectively, 11 mM/l, were considered. The “shots” were taken at the same moment in time. As it can be observed the tendency of spiral wave formation is decreased as ischemia advances. Experimental measurements of extracellular potassium concentration during acute ischemia [16] suggest that the dangerous initial phase we observed is situated within the first 5 min of coronary occlusion. As a consequence, a proper detection of this phase might be crucial for the patient’s life. In order to investigate the possibility of this early detection, as well as other changes related with different phases of ischemia, the theoretical ECG was reconstructed [4]. The three lead ECG signal “recorded” from our 2-D model of myocardium during normal conditions can be seen in Fig. 9. The abscissa shows the simulated “real” time evolution in ms, while the *y*-axis is presented in arbitrary units. First observation that should be made is the missing of *P*-wave. As we modeled the ventricular myocardium, the atrial depolarization is not “recorded” in the ECG signal. The *T* wave attributed by others [26] to different epicardial/endocardial repolarization durations is generated in our case by the differences in repolarization moments over the sur-

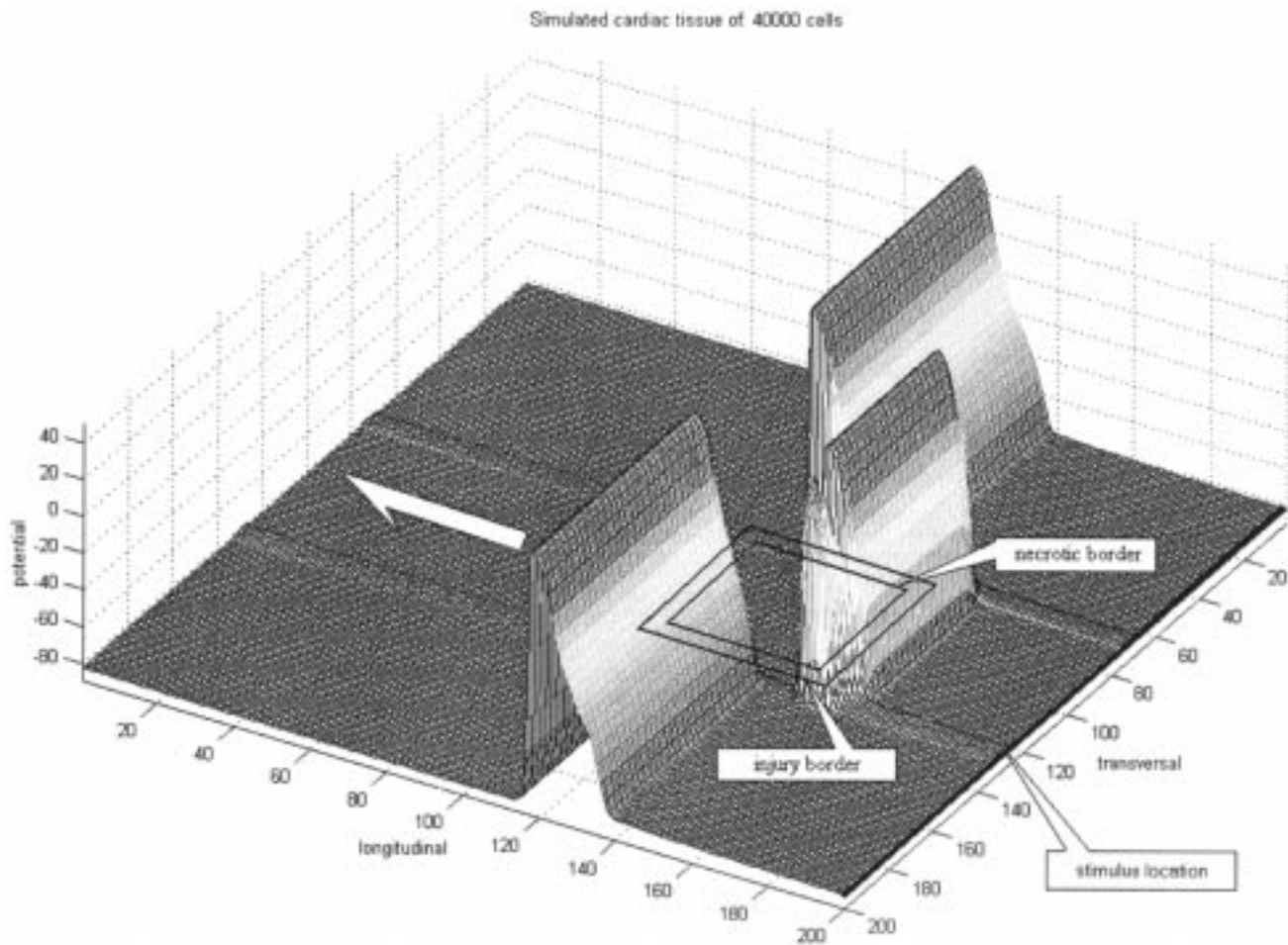


Fig. 7. Simulation of infarction in the 2-D model.

face of the tissue [24]. Leads I and II show a negative deflection of the *R* peak and positive one for the *T* wave, while in lead III the *R* peak has positive deflection. For the first beat, the simulated myocardium was in total resting state. The next beats show slightly higher peak amplitude due to the residual charge that is not able to flow out at the far-end boundary. However, this effect was greatly reduced by using the reconstruction technique mentioned in the methods section, and affecting uniformly all the following beats, does not alter the accuracy of the simulation.

The acute ischemic conditions were induced in the 2-D model using a homogeneous distribution of hyperkalemia over the 2-D sheet. The analysis demonstrated an increased propagation velocity in the first moments of ischemia. We mentioned already, that the origin of this phenomenon is an increased excitability of the ischemic cell in the first few minutes of coronary occlusion, demonstrated by the cellular analysis. ECG computation for 7-mM/l hyperkalemia was performed in order to probe a similar effect in the ischemic myocardial tissue and find out how this phenomenon can be detected. Fig. 10 shows a significant increase in QRS peak amplitude in all the three leads when comparing with the normal myocardium. Computing the ECG for 9-mM/l (Fig. 11) and 11-mM/l (Fig. 12) hyperkalemia we can see that the observed decreased cellular excitability manifesting as acute ischemia advances, leads to gradual decrease of

QRS complex amplitude. This transient increase in QRS complex amplitude during acute ischemia, followed later by a continuous decrease of the same parameter, constitute a good basis for clinical detection of the two already mentioned phases of acute ischemia.

The QRST region of the ECG shows during acute ischemia, deformations in all the three leads due to disturbances in excitability and abnormal repolarization. The ST segment duration is reduced mainly in response to changes in AP duration in the same direction. At high levels of hyperkalemia, this effect is accompanied by the elevation of ST segment leading in the advanced phase to QRS complex and *T* wave overlap (Figs. 11 and 12). The displacement occurs above or below the zero-potential line, function of the analyzed lead (positive shift for leads I and II, and negative one for lead III, in our simulations).

At high $[K^+]_{out}$ values the *T* wave becomes higher and pointed (Figs. 11 and 12). This observation comes into agreement with clinical recordings of ECG during ischemia [27]. A clear explanation, however, for this phenomenon was not formulated. As the *T* wave corresponds to ventricular repolarization, the dramatic changes in potassium concentration during advanced phases of acute ischemia strongly disturb the membrane return to resting state. On the other hand the absence of epicardial/endocardial cells in our model makes this alterations difficult to interpret and the conclusions might not

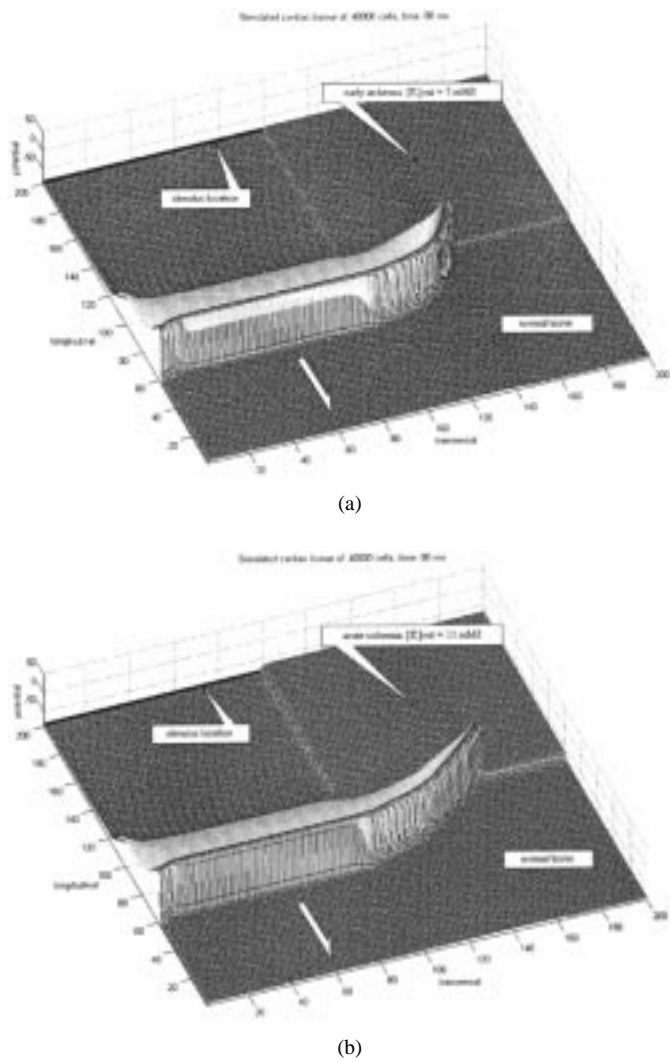


Fig. 8. Wave propagation in the simulated myocardium partially affected by ischemia.

be the most accurate. However, detection of these changes is motivated by observation that during this period the Na^+ channels recover from inactivation, changes in T wave morphology proving to be clear signs of cardiac instability [3].

An additional observation can be made after a direct comparison of lead III in normal myocardium (Fig. 9) and for $[\text{K}^+}_{\text{out}} = 11 \text{ mM/l}$ (Fig. 12). The QRS complex becomes wider as hyperkalemia advances. The origin of QRS complex is the membrane depolarization or initiation phase of the AP. We observed in the cellular study that the up-stroke velocity, in other words the slope of AP's phase 0, decreases significantly in the advanced phase of acute ischemia. So, we think we can correctly emphasize here that the widening of the QRS complex is not the result of conduction disturbance at tissue level as a consequence of structural changes (the cell-to-cell uncoupling does not occur in this phase), but merely the consequence of decreased AP up-stroke velocity associated with cellular excitability decrease. As we pointed out earlier the lost of excitability favors also the decrease of propagation velocity which in turn can be detected in the ECG from the widening of QRS complex.

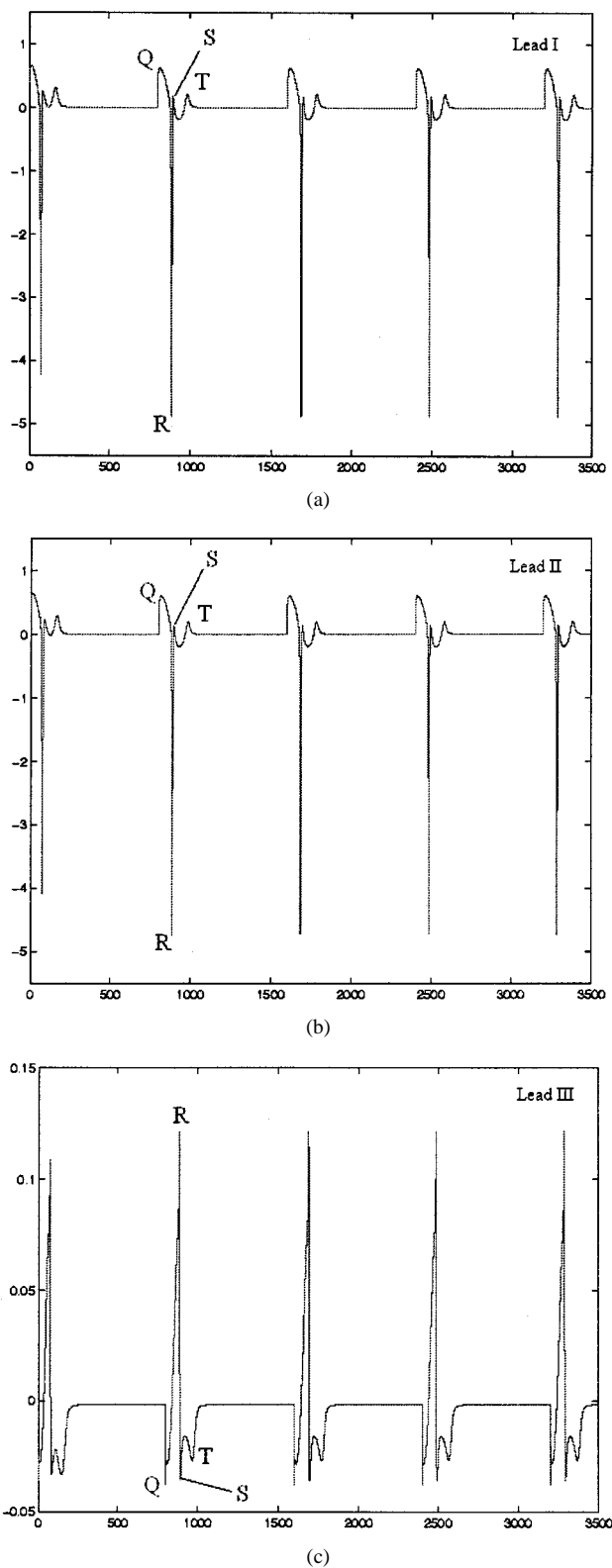
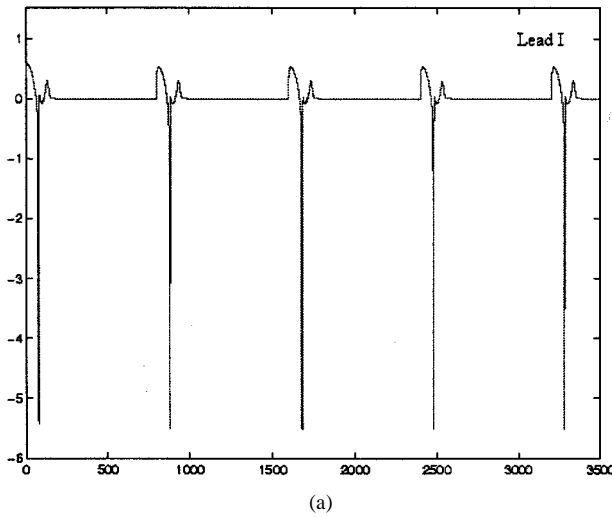
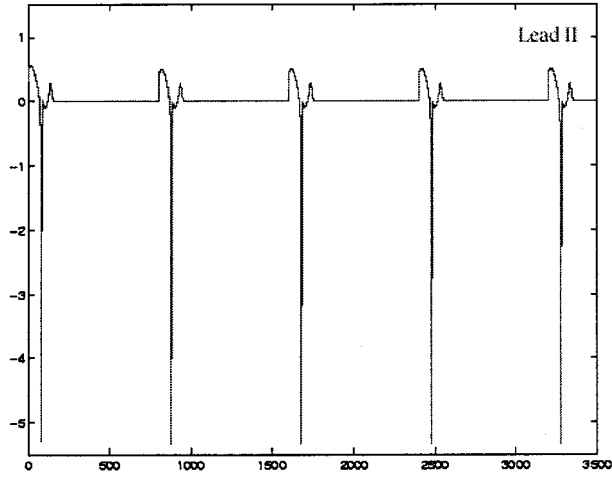


Fig. 9. Reconstructed three-lead ECG from the normal myocardium.

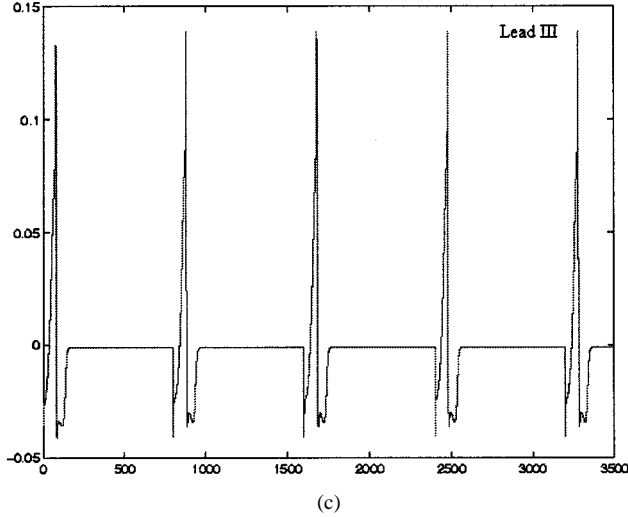
It is clearly seen, especially in the lead III that as ischemia advances, an enlarged Q manifested. It was clinically observed that the ECG recording on patients suffering of acute ischemia, shows enlarged Q waves [27] starting from the first hour of coronary occlusion, phenomenon that may be clearly visible even after many years have passed from the coronary attack. We do



(a)



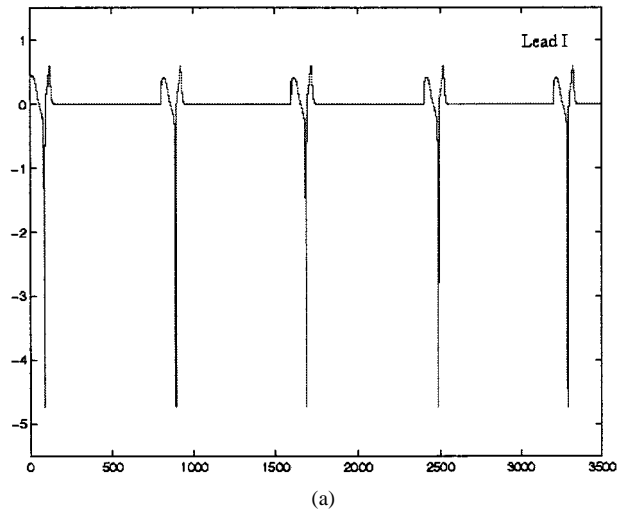
(b)



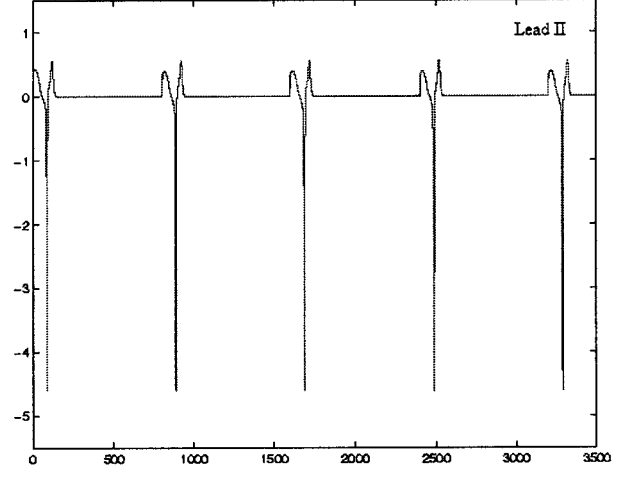
(c)

Fig. 10. Reconstructed ECG during early ischemia ($[K]_{out} = 7 \text{ mM/l}$).

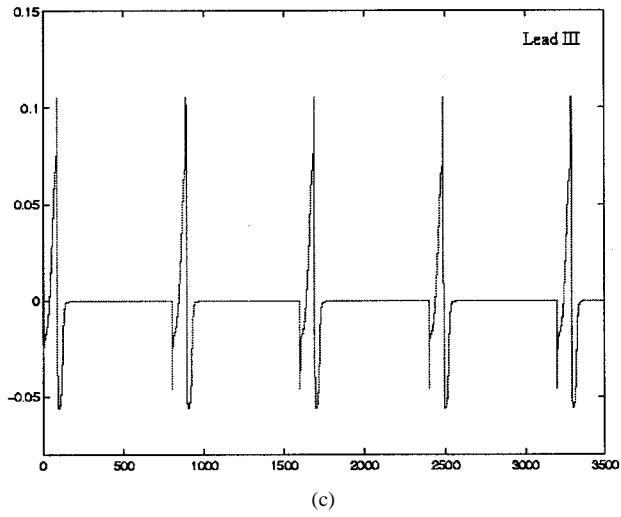
not have a certain explanation of the phenomenon, but it might be related with the time response delay of the sodium channels as the *Q* wave corresponds to the initiation phase of the AP. As we observed, the sodium time response is improved during acute ischemia and the faster reaction of the membrane may create the



(a)



(b)



(c)

Fig. 11. Reconstructed ECG during acute ischemia ($[K]_{out} = 9 \text{ mM/l}$).

spike-like *Q* wave. However, the sodium amplitude response suffers an opposite tendency, degrading gradually as ischemia advances. So, as it can be seen in lead III recording from Fig. 12, despite of the enlarged *Q*, the QRS complex amplitude drops dramatically at high levels of hyperkalemia.

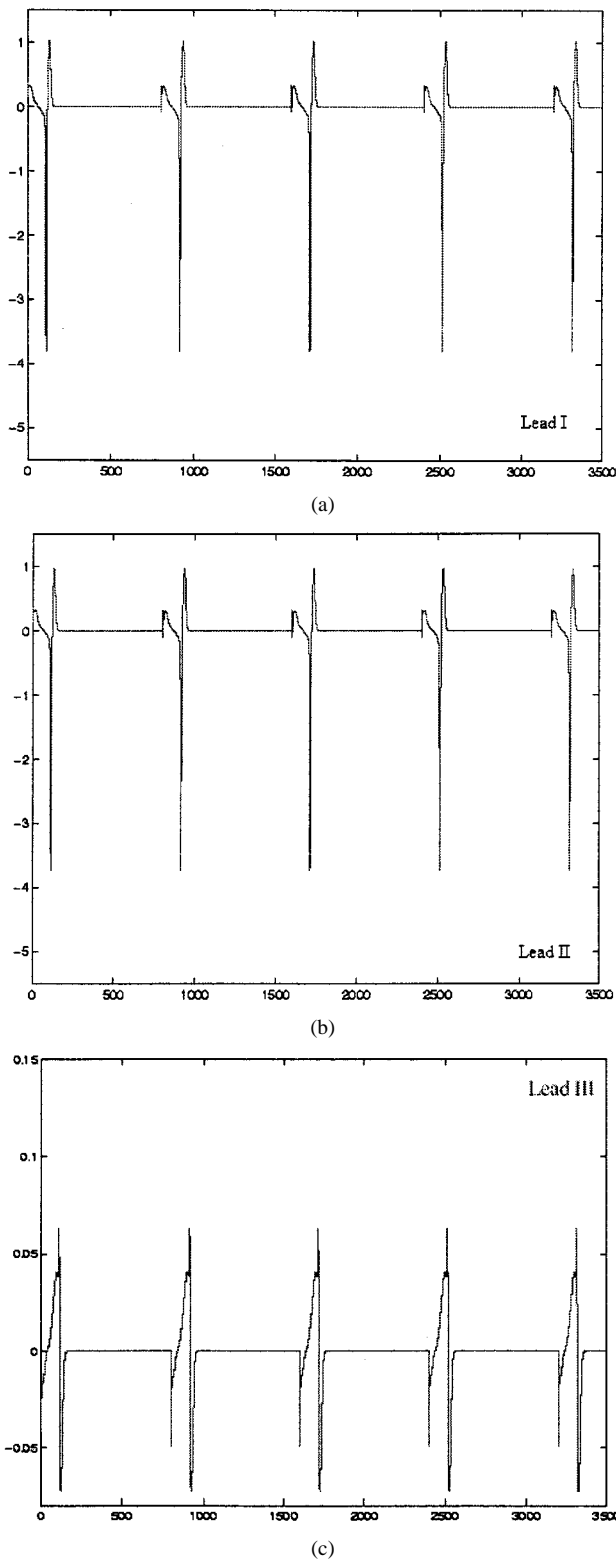


Fig. 12. Reconstructed ECG during acute ischemia ($[K]_{out} = 11 \text{ mM/l}$).

In order to analyze the propagation during infarction, a 200×200 cells simulated tissue was considered. The infarcted area was defined as a 40×40 cells region uncoupled from the normal tissue by high-resistance gap-junction connections (one order of magnitude higher than in normal tissue). In order to have a more realistic representation a five cells width transitional band, surrounding the necrotic area, was considered. The gap-

junction resistance employed for this surrounding region is a mid-way value between the normal ($200\text{-}\Omega\cdot\text{cm}$ effective value) and necrotic one ($2\text{-k}\Omega\cdot\text{cm}$ effective value). This representation is close to real infarcted myocardium where the necrotic region is surrounded by injured tissue. Conduction in this structure was implicitly affected by the gradual increase in axial resistance as the depolarization wave reaches the injured region border. The propagation velocity drops suddenly in this area and part of the depolarization wave manifests considerable delay, leading to gradual separation and wave fragmentation (Fig. 7). This creates proper conditions for spiral wave formation (not shown), as the broken parts separate from the obstacle. Evidence exists [6] concerning a direct relationship between the transitional border (injured tissue) width and wave break as the separation takes place within this boundary layer as it can be seen in our simulation (Fig. 7). The two squares in Fig. 7 show the limits of the necrotic region and injury band and their position relative to 2-D structure as they were used during the simulations.

The induced nonuniform spatial distribution in gap-junction resistance combined with altered ion concentrations creates potential differences between different regions of the 2-D layer. This gives rise to “injury currents” flowing across the infarcted myocardium. ECG reconstruction reflects the propagation disturbances by showing alteration of all characteristic waves pattern (Fig. 13). The polymorphic changes present in the reconstructed signal account on tissue re-excitation by “injury currents” [24] and the consequent spiral waves formation [4], [28] due to re-entry. Proarrhythmic tendency becomes evident, the ECG showing signs of ectopic beats occurrence especially in leads I and II. The ST segment is deflected above or under the base line due to injury potential of the damaged area, affecting the whole QRST region conformation.

A post-infarction “recording” was performed to identify persistent alterations of heart electrophysiology after myocardial impairment. The three-lead ECG was computed (Fig. 14) considering normal chemical concentrations on a partially damaged myocardium (Fig. 7), mimicking the resolving period of infarction. More specific, we preserved the structural alterations (different gap-junction resistance for normal, necrotic and transitional border areas, as presented above) using the normal values for channels conductivities and ion concentrations. We found that the ST segment level is the first to return to normal in the absence of chemical disturbances. However, abnormal *T* wave still manifests, displaying stubborn abnormal repolarization. During acute phase of ischemia, we probed the clinically observed enlarged *Q* wave. As it was already mentioned, indications exist that the phenomenon can be observed even after years passed from the infarction. Simulations performed on our model prove this phenomenon, more evident in the reconstructed lead III. Overall, the function of the myocardium is recovered satisfactory, the remaining alterations showing a shift from polymorphism to monomorphic changes.

IV. DISCUSSION AND CONCLUSIONS

In this study we employed a simple yet realistic, cellular formulation to study the electrical activity of both acute and chronic

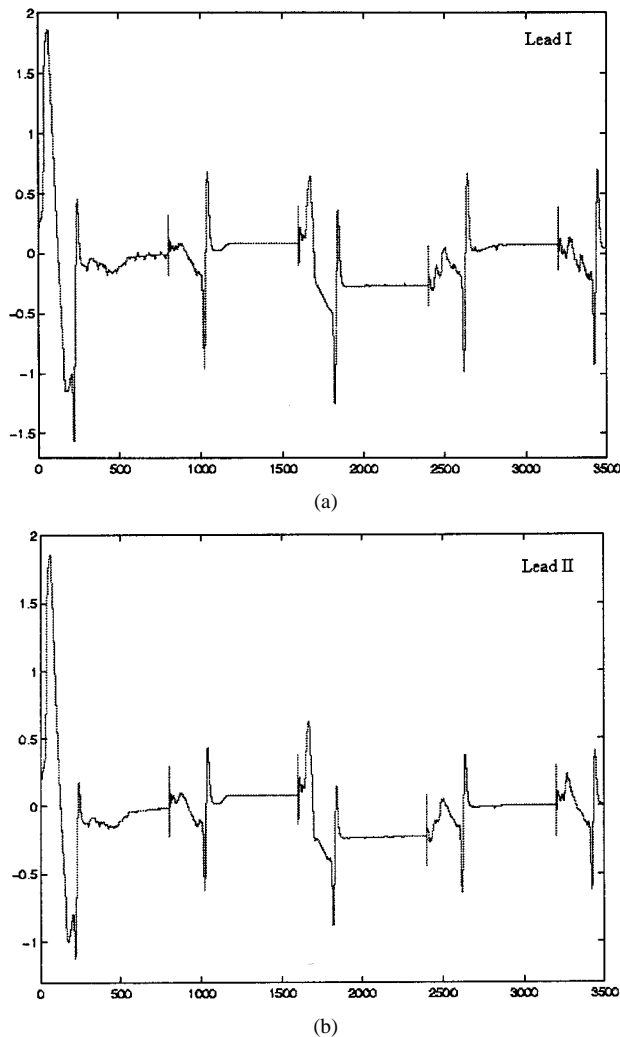


Fig. 13. Theoretical ECG reconstructed during simulated myocardial infarction.

ischemic heart using a 2-D model of the myocardium. The relative simplicity of the cellular model allowed computations on relatively large 2-D structures (200×200 cells). A cellular analysis was performed with double purpose: to validate the capacity of the model in simulating pathological conditions and link the 2-D results with microscopic changes. All the three main characteristics of ischemia were investigated. The results are similar with those obtained in other studies using the LR II cellular model [19] proving that LR I model has the potential to provide accurate results in studying pathological conditions. The lack of ATP-sensitive potassium current in this model gave us slightly different results concerning the AP duration, attributed to the associated channels under hypoxic conditions. However, the dramatic reduction in APD proved by animal experiments using pharmacological opening of these channels [29], cannot be used in our opinion as motivation for modeling hypoxia induced opening of these channels as there is no clear evidence that K_{ATP} channels open during acute ischemia [17], [18].

Some differences were also obtained for the hyperkalemic depolarization of the membrane during early phase of simulated coronary occlusion. A baseline membrane potential around -60 mV was suggested after some 7 min of continuous ischemia

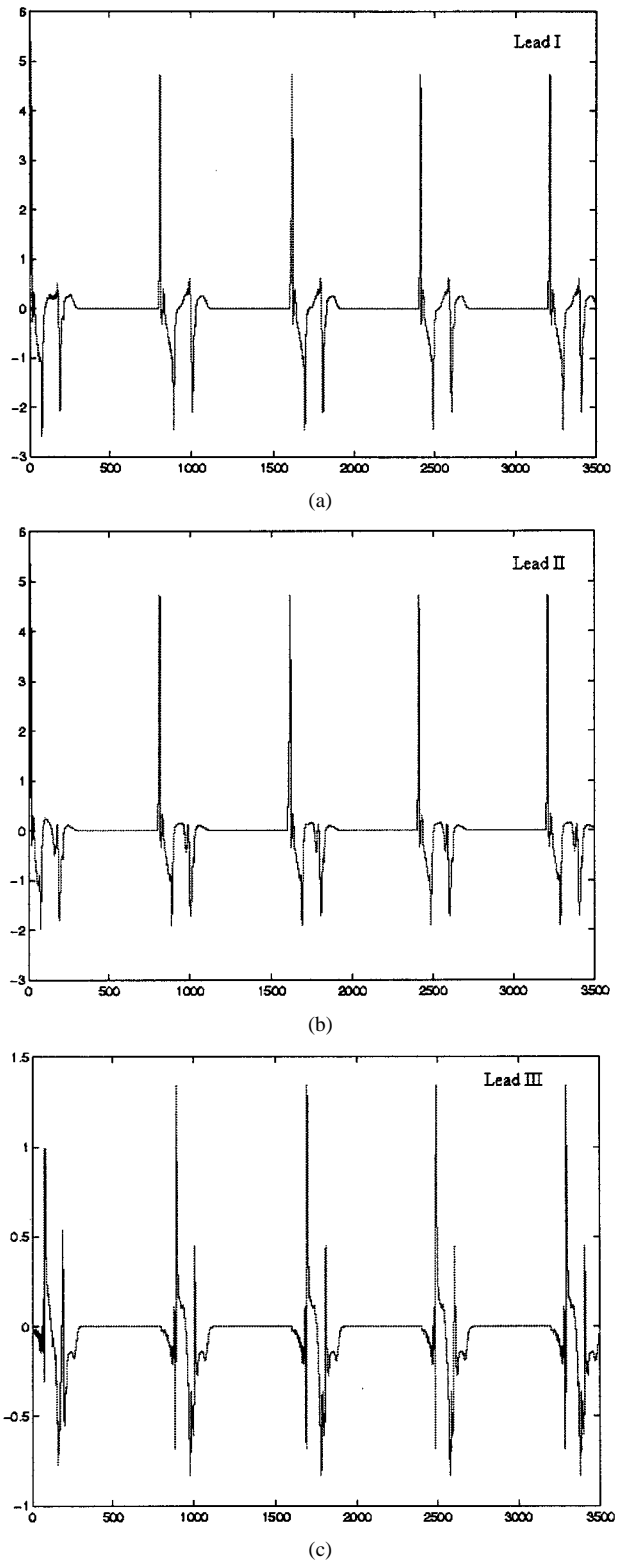


Fig. 14. Theoretical ECG reconstructed from the simulated infarcted myocardium after resolving.

when $[K^+]_{out}$ is situated around an 8-mM/l value [15]. Our results show lower degree of depolarization for that level of hyperkalemia. It might be suggested that the 5- to 10-mV difference accounts for the malfunctioning of the Na^+-K^+ pump which loses the ability to extrude the corresponding ions, with direct effect on membrane potential. However the experimental

results concerning pump's activity during acute ischemia are contradictory [8], [15]. Kleber's study on guinea pig hearts [16] suggesting that during the first 10–15 min of coronary occlusion, the $\text{Na}^+ \text{-K}^+$ pump continues to function in a relatively normal manner. Since the LR model accounts for data taken from guinea pig, we support the comparison with Kleber's work.

Clinical comparison was supported by the theoretical reconstruction of the three-lead ECG signal. At each step, we tried to clarify the origin of electrical changes in the frame of forward problem, pointing out the necessary elements for detecting the unique solution when dealing with inverse problem of electrocardiography [30]. In the acute ischemia analysis we were able to distinguish between two phases of altered electrophysiology: an early phase characterized by increased excitability and decreased refractoriness, and a delayed phase showing opposite tendencies. These stages correspond quite accurate to the two phase-occurrence of life threatening arrhythmias in canine acute ischemic hearts [15]. The first phase, "type 1a" or "immediate", has a peak incidence of 5–6 minutes, while the second one, "type 2b" or "delayed" has its maximum occurrence probability around 15–20 min after coronary occlusion [8]. While for the first stage we were able to detect the origin of phase 1a arrhythmia in the tissue vulnerability to reentry, for the second stage we did not find a phenomenon that might be responsible for generating the delayed arrhythmias, as this phase shows a relative electrical stability, characterized by a gradual loss of cell excitability, reported also experimentally [8], [15]. However, the exact mechanism for ventricular delayed arrhythmias in the second phase is not known [8]. In the ECG, changes in ST segment and *T* wave characteristics permitted to detect the presence of ischemia. Early stage was identified by the transient increase in QRS complex amplitude, while the advanced phase was distinguished by decreased QRS amplitude, widening of QRS complex and enlarged *Q* wave. These observations give a good basis for prompt detection of acute ischemia and necessary counteracting actions that should be taken according to the identified stage. The results encourage further studies on theoretical analysis of ischemia treatment using modeled drug action, currently under our attention.

Polymorphic changes in the reconstructed ECG were identified to have the origin in irreversible changes associated with infarction. Non-uniform deflection of the ST segment in our simulations played a major role in the ECG morphology associated with infarction and were attributed to flowing of injury currents from the damaged area of the myocardium to normal tissue regions. Relative restoring of ventricular function was identified in the theoretical ECG computed from simulated tissue after resolution of the acute phase of infarction. The restoration of the baseline of the ECG proves that the ST segment deflection is directly related with chemical alteration and not with the structural changes at tissue level. This is in accordance with explanations of ST segment elevation during acute ischemia formulated in [26] and suggests an injury current based deflection. Our acute ischemia ECG reconstruction did not imply a nonuniform distribution of the chemical alteration and thus cannot rely on this explanation of ST elevation. On the other hand such assumption of nonuniform distribution

of ischemia over the analyzed tissue would also give a polymorphic ECG which is not likely to be obtained during continuous acute ischemia [27], [31]. In the early phase, however, such nonhomogeneous chemical alteration might be present as it is proved by the experimental analysis of ischemia-induced arrhythmias [8]. We do not have however clinical information concerning the shape of the ECG during this phase mainly because the occurrence duration is very short (5–6 min). New clinical data are expected in order to clarify this problem. Also further investigation of the still controversial mechanisms of tissue revascularization after infarction and their monitoring in the ECG is necessary in order to identify the proper moment of applying this promising technique.

ACKNOWLEDGMENT

The authors would like to thank the Medical University of South Carolina for their continuing support.

REFERENCES

- [1] R. Ferrari, "A symposium: Metabolic management of ischemic heart disease," *Amer. J. Cardiol.* 82, Sept. 3, 1998. Introduction.
- [2] N. Maglaveras, F. J. L. van Capelle, and J. M. T. De Bakker, "Wave propagation simulation in normal and infarcted myocardium: Computational and modeling issues," *Med. Informatics*, vol. 23, no. 2, pp. 105–118, 1998.
- [3] C. F. Starmer, A. R. Lancaster, A. A. Lastra, and A. O. Grant, "Cardiac instability amplified by use-dependent Na channel blockade," *Amer. Physiol. Soc.*, pp. H1305–H1310, 1992.
- [4] C. F. Starmer, D. N. Romashko, R. S. Reddy, Y. I. Zilberman, J. Starobin, A. O. Grant, and V. I. Krinsky, "Proarrhythmic response to potassium channel blockade—Numerical studies of polymorphic tachyarrhythmias," *Circulation*, vol. 92, no. 3, pp. 595–605, 1995.
- [5] N. Maglaveras, F. Offner, F. J. L. van Capelle, M. A. Allessie, and A. V. Sahakian, "Effects of barriers on propagation of action potentials in two-dimensional cardiac tissue—A computer simulation study," *J. Electrophysiol.*, vol. 28, no. 1, pp. 17–31, 1995.
- [6] J. M. Starobin and C. F. Starmer, "Boundary-layer analysis of waves propagating in an excitable medium: Medium conditions for wave-front-obstacle separation," *Phys. Rev. E*, vol. 54, no. 1, pp. 430–437, 1996.
- [7] A. T. Winfree, "Varieties of spiral wave behavior: An experimentalist's approach to the theory of excitable media," *Chaos* 1, pp. 303–334, 1991.
- [8] F. A. Ehlert and J. J. Goldberger, "Cellular and pathophysiological mechanisms of ventricular arrhythmias in acute ischemia and infarction," *Pacing Clin. Electrophysiol.*, vol. 20, no. 4, pp. 966–975, 1997.
- [9] C. Lou and Y. Rudy, "A model of the ventricular cardiac action potential. Depolarization, repolarization, and their interaction," *Circ. Res.*, vol. 68, pp. 1501–1526, 1991.
- [10] C. H. Lou and Y. Rudy, "A dynamic model of the cardiac ventricular action potential. I. Simulations of ionic currents and concentration changes," *Circ. Res.*, vol. 74, pp. 1071–1096, 1994.
- [11] ———, "A dynamic model of the cardiac ventricular action potential—II: Afterdepolarizations, triggered activity, and potentiation," *Circulation Research*, vol. 74, pp. 1097–1113, 1994.
- [12] E. Neher and B. Sakmann, "The patch clamp technique," *Scientific American*, vol. 266, no. 3, pp. 28–35, 1992.
- [13] W. Quan, S. J. Evans, and H. M. Hastings, "Efficient integration of a realistic two-dimensional cardiac tissue model by domain decomposition," *IEEE Trans. Biomed. Eng.*, vol. 45, pp. 372–385, Mar. 1998.
- [14] A. L. Hodgkin and A. F. Huxley, "A quantitative description of membrane current and its application to conduction and excitation in nerve," *J. Physiol.*, vol. 117, pp. 500–544, 1952.
- [15] D. P. Zipes and J. Jalife, *Cardiac Electrophysiology—From Cell to Bedside*, 2nd ed. Philadelphia, PA: Saunders, 1995.
- [16] A. G. Kleber, "Resting membrane potential, extracellular potassium activity and intracellular sodium activity during acute global ischemia in isolated perfused guinea pig hearts," *Circ. Res.*, vol. 52, pp. 442–450, 1983.

- [17] S. Shigematsu and M. Arita, "Anoxia-induces activation of ATP-sensitive K^+ channels in guinea pig ventricular cells and its modulation by glycolysis," *Cardiovasc. Res.*, vol. 35, no. 2, pp. 273–282, 1997.
- [18] G. X. Yan, K. A. Yamada, A. G. Kleber, J. McHowat, and B. B. Corr, "Dissociation between cellular K^+ loss, reduction in repolarization time, and tissue ATP levels during myocardial hypoxia and ischemia," *Circ. Res.*, vol. 72, pp. 560–570, 1993.
- [19] R. M. Shaw and Y. Rudy, "Electrophysiologic effects of acute myocardial ischemia: A theoretical study of altered cell excitability and action potential duration," *Cardiovasc. Res.*, vol. 35, pp. 256–272, 1997.
- [20] B. Alberts *et al.*, *Molecular Biology of the Cell*, 3rd ed. New York: Garland, 1994.
- [21] A. G. Loevy, P. Siekevitz, J. R. Menninger, and J. A. N. Gallant, *Cell Structure & Function—An Integrated Approach*, 3rd ed. Philadelphia, PA: Saunders College, 1991.
- [22] N. Maglaveras, J. M. T. De Bakker, F. J. L. van Capelle, C. Papas, and M. J. Janse, "Activation delay in healed myocardial infarction: A comparison between model and experiment," *Amer. Physiological Soc.*, pp. H1441–H1449, 1995.
- [23] A. V. Sahakian, G. A. Myers, and N. Maglaveras, "Unidirectional block in cardiac fibers: Effects of discontinuities in coupling resistance and spatial changes in resting membrane potential in a computer simulation study," *IEEE Trans. Biomed. Eng.*, vol. 39, pp. 510–522, May 1992.
- [24] R. M. Berne and M. N. Levy, *Physiology*. Washington, D.C.: Mosby, 1988.
- [25] A. Cimponeriu, C. F. Starmer, and A. Bezerianos, "Action potential propagation in ischemic cardiac tissue: A theoretical computer modeling," in *Comput. Cardiol.*, vol. 25. Cleveland-Ohio, OH, 1998, pp. 317–320.
- [26] I. Cohen, W. Giles, and D. Noble, "Cellular basis for the T wave of the electrocardiogram," *Nature*, vol. 262, no. 5570, pp. 657–661, 1976.
- [27] A. Despopoulos and S. Silbernagl, *Color Atlas of Physiology*, 4th ed. New York: Thieme Medical, 1991.
- [28] C. F. Starmer and J. Starobin, "Spiral tip movement: The role of the action potential wavelength in polymorphic cardiac arrhythmias," *Int. J. Bifurcation Chaos*, vol. 6, no. 10, pp. 1909–1923, 1996.
- [29] T. M. Mouticello, C. A. Sargent, J. R. McGill, and D. S. Barton, "Amelioration of ischemia/reperfusion injury in isolated rat heart by the ATP-sensitive potassium channel opener BMS-180448," *Cardiovasc. Res.*, vol. 31, no. 1, pp. 93–101, 1996.
- [30] R. M. Gulrajani, "The forward and inverse problems of electrocardiography," *IEEE Eng. Med. Biol. Mag.*, vol. 17, no. 5, pp. 84–101, 1998.
- [31] N. Sperelakis, *Cell Physiology—Source Book*. New York: Academic, 1995.



Adrian Cimponeriu received the B.S. degree in applied electronics from the "Politehnica" University of Timisoara, Timisoara, Romania, in 1994 and the M.S. degree in biomedical engineering from the University of Patras, Patras, Greece, in 1999. He is currently working as a Ph.D. fellow at the Department of Medical Physics, University of Patras, Greece.

His current research focuses on cardiac modeling, ischemia and antiarrhythmic drugs effects.



C. Frank Starmer is currently Associate Provost for Information Technology at the Medical University of South Carolina, Charlesto, SC. Prior to this, he was Professor of Medicine (Cardiology) and Professor of Computer Science at Duke University, Durham, NC. The work reported in this paper was initiated while he was a Fulbright Scholar at the University of Patras, Patras, Greece. For additional biographical information, visit: <http://www.musc.edu/~starmer/>.



Anastasios Bezerianos was born in Patras, Greece, in 1953. He received the B.Sc. degree in physics from Patras University in 1976, the M.Sc. degree in telecommunications and electronics from Athens University, Athens, Greece, and the Ph.D. degree in medical physics from Patras University.

He is currently an Associate Professor with the Medical School of Patras University. His main research interests are concentrated in biomedical signal processing and medical image processing—data acquisition and on line processing using digital

signal processors, nonlinear time series analysis of electrocardiogram, wavelet analysis of high-resolution electrocardiogram, modeling of heart muscle and heart rate variability, wavelet analysis of medical images, and cinecardiographic image analysis. His research activities are summarized in three books, 60 scientific publications and many conference publications.